

## Autodetachment Dynamics of Acrylonitrile Anion Revealed by Two-Dimensional Electron Impact Spectra

K. Regeta and M. Allan

*Department of Chemistry, University of Fribourg, Chemin du Musée 9, CH-1700 Fribourg, Switzerland*

(Received 15 March 2013; published 13 May 2013)

Two-dimensional electron energy-loss spectra of acrylonitrile are presented in the incident energy range 0.095–0.9 eV, where the incoming electron is temporarily captured in the lowest  $\pi^*$  orbital. The cross section is plotted as a function of the incident electron energy that determines which vibrational resonant anion state is populated, and of the electron energy loss, that shows into which final vibrational states each resonance decays. The striking result is that besides the expected horizontal (for given resonances) and vertical (for given final states) patterns of peaks, diagonal arrangements of peaks are observed. They reveal restrictive selectivity with respect to which vibrations are deexcited in the detachment process, with  $\nu_4$  (C $\equiv$ N stretch) and  $\nu_7$  (C—H rocking) dominating. Surprisingly, all spectral features could be assigned to vibrational levels of the valence  $\pi^*$  resonance, and none to dipole-bound vibrational Feshbach resonance, although the latter must also exist in this energy range.

DOI: [10.1103/PhysRevLett.110.203201](https://doi.org/10.1103/PhysRevLett.110.203201)

PACS numbers: 34.80.Gs, 52.20.Fs

The interplay of nuclear and electronic motion in the autodetachment of transient molecular anions is a fascinating subject and the emitted electron carries information about the motion of the nuclei on the anion potential surface. Autodetachment may proceed with several different mechanisms, depending on the nature of the anion and its energy relative to the neutral molecule [1,2]. One of them, vibrational autodetachment, is a prototype process where the Born-Oppenheimer approximation is broken. One approach to the experimental study of autodetachment is based on vibrational photoexcitation of bound anions and detection of autodetached electrons [3–8], but the autodetaching anions can also be formed by electron attachment [9,10]. Various aspects of the theory were explained in the work of Simons [2,11–13], with emphasis on vibrational autodetachment that requires inclusion of non-Born-Oppenheimer coupling, the theory of which has initially been inspired by the work on the related process of vibrational autoionization [14].

In this work we prepare the anions by attachment of free electrons, but substantially enhance the power of this method by recording a two-dimensional (2D) electron impact spectrum where cross section, represented by color, is plotted as a function of the incident electron energy, which determines the initial state of the negative ion, and of the energy loss, which carries information about the final state of the neutral molecule. This spectrum yields complete information about the decay channels of many resonances. Two-dimensional electron spectra were used in the past to study N<sub>2</sub> [15] and CO<sub>2</sub> [16].

Acrylonitrile CH<sub>2</sub>CHCN is a suitable target for this study because electron transmission spectroscopy (ETS) revealed sharp structures—narrow resonances—in electron scattering at low energy [17]. Another interesting aspect of acrylonitrile in connection with the present work is that its

large dipole moment (3.86 D) supports a dipole-bound state, with a measured binding energy of 6.9 meV [18–21]. Acrylonitrile thus potentially offers the possibility to study the coexistence of, and interactions between, the dipole-bound and the valence states of an anion [22,23]. Dissociative electron attachment for acrylonitrile has been measured [24]—the lowest bands have an onset around 2 eV, above the energy range of the present work. The interest in acrylonitrile is augmented by its occurrence in outer space [25] where it may be exposed to free electrons, and because it is a widely used monomer precursor in polymer science.

*Methods.*—The measurements were performed using a spectrometer with hemispherical analyzers [26]. The energy scales are accurate to within  $\pm 10$  meV; the resolution was 16 meV in the energy-loss mode with a 300 pA beam current. The 2D spectrum was obtained by recording a series of 160 electron energy-loss (EEL) spectra with constant incident energies in the range 0.095–0.9 eV and combining them to a 2D spectrum. Each of the 160 EEL spectra was corrected for the response function of the analyzer and then arbitrarily normalized to 1 at the top of the elastic peak. Since the elastic peak drops with rising incident energy in reality, normalizing it to 1 enhances somewhat the signal at higher incident energies, and improves visibility. Spectra were recorded at the scattering angle of 135° to emphasize resonant processes and reduce the extent of direct excitation in the spectrum. All calculated quantities given in this Letter were obtained with density functional theory at the B3LYP/6–311 + +G(2df, 2p) level, with the FIREFLY code [27], based partly on GAMESS [28].

*Results.*—The 2D EEL spectrum shown in Fig. 1 plots the differential cross section, represented by color, as a function of the electron energy loss  $\Delta E$  and of the

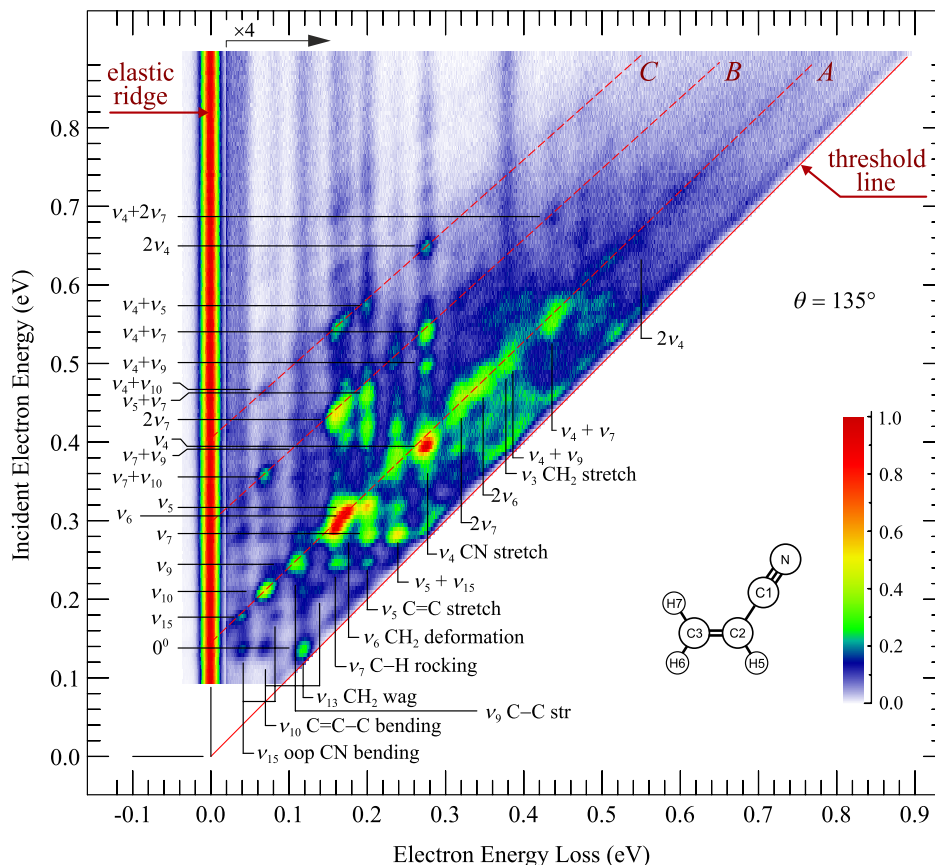


FIG. 1 (color online). Two-dimensional electron energy-loss spectrum of acrylonitrile.

incident electron energy  $E_i$ . The elastic peak has  $\Delta E = 0$  and gives rise to the red vertical ridge on the left. The largest possible  $\Delta E$  is equal to  $E_i$  for each incident energy and corresponds to the situation where all the energy of the incident electron is used for internal excitation of the acrylonitrile target and the electron leaves with nearly zero kinetic energy. At this point the excitation of the final state is at its threshold and this situation is encountered along the diagonal threshold line drawn red in Fig. 1.

Excitation of a given final vibrational state of the neutral acrylonitrile occurs at a given  $\Delta E$  for various  $E_i$  and gives thus rise to a group of peaks (dots) arranged vertically at the corresponding energy loss. The excitation is predominantly resonant, and since acrylonitrile is known to have narrow structures of vibrational origin in the lowest  $\pi^*$  shape resonance [17], the cross section has peaks at the discrete energies of the resonances. A given resonance (vibrational state of the transient acrylonitrile anion) decays, with some selectivity, into various vibrations, and these decay channels give rise to a group of peaks (dots) arranged horizontally at the incident energy equal to the energy of the resonance.

The two expected features in the 2D spectrum in Fig. 1 are thus vertical rows of dots, with each row corresponding

to a given final vibrational state, and horizontal rows of dots, with each row corresponding to a given resonance. The striking observation of this Letter is the patterns of diagonally arranged dots. The three most prominent diagonal rows are marked by the red dashed lines A, B, C in Fig. 1. The rows are nearly, but not exactly, parallel to the threshold line, slowly approaching it with increasing  $E_i$ . A quantity common to all dots on a given diagonal is their horizontal shift from the threshold line—it is the residual energy of the scattered electron  $E_r = E_i - \Delta E$ . The diagonal groups of peaks thus reveal a propensity for discrete residual energies. This is unexpected because residual energy is not directly related to either of the two important quantities of the present experiment—energy of a resonance and energy of the final state.

*Assignment of the final vibrational states.*—The assignment of the individual vibrations is indicated by vertical bars and labels in the lower part of Fig. 1. The bars are drawn at energy losses equal to the vibrational frequencies of neutral acrylonitrile [29]. The  $\pi^*$  orbital where the incoming electron is temporarily captured is antibonding with respect to the  $C\equiv N$  and  $C=C$  bonds, making them longer and reducing the vibrational frequencies (see Table I), thus providing a force for excitation of  $\nu_4$  and  $\nu_5$ , explaining their prominence in Fig. 1. The

TABLE I. Observed [29] and calculated (scaled by a factor of 0.97) vibrational frequencies of acrylonitrile and its anion (in meV).

No.	Sym	Type	Neutral molecule		Anion
			Observed	Calculated	Calculated
$\nu_1$	$A'$	(C—H) asym. str of CH <sub>2</sub>	387	392	387
$\nu_2$		(C—H) str of C—H	382	382	377
$\nu_3$		(C—H) sym. str of CH <sub>2</sub>	377	378	376
$\nu_4$		C≡N str	278	280	257
$\nu_5$		C=C str	200	201	179
$\nu_6$		CH <sub>2</sub> scissoring	176	174	168
$\nu_7$		C—H rock	159	159	146
$\nu_8$		CH <sub>2</sub> rock	136	134	131
$\nu_9$		C—C str	108	106	107
$\nu_{10}$		C=C—C bend	n.o.	70.2	72.0
$\nu_{11}$		C—C≡N bend	28.4	29.2	28.9
$\nu_{12}$	$A''$	C—H wag (C2 pyram)	121	121	69.5
$\nu_{13}$		CH <sub>2</sub> wag (C3 pyram)	118	120	24.7
$\nu_{14}$		C=C torsion (C2 pyram)	84.7	85.7	59.6
$\nu_{15}$		oop C—C≡N bend	41.3	42.0	39.3

lowering of the frequencies  $\nu_6$  and  $\nu_7$  in the anion (see Table I) also indicates a change of bonding along these modes and rationalizes their substantial intensity in the spectrum. The appreciable intensity of the  $A''$  out-of-plane (oop) vibrations is initially not understandable because both acrylonitrile and its anion are calculated to be planar. The dramatic lowering of the frequencies  $\nu_{12}$  and  $\nu_{13}$  (unresolved in the spectrum) indicates that the acrylonitrile anion is ‘on the verge of becoming pyramidal’ on the C2 and C3 carbons (see the insert in Fig. 1 for numbering); the potential curves along these two modes become flat in the anion, and this change drives the vibrational excitation.

*Assignment of resonances.*—Assignment of the resonances is indicated on the left of Fig. 1. It was obtained by finding a match of the observed spectral features with the calculated vibrational frequencies of the acrylonitrile anion listed in Table I. The energy of the origin of the anion vibrational grid is the adiabatic electron attachment energy of acrylonitrile and is *a priori* not known. To determine it, the calculated vibrational grid was moved along the vertical axis until a good match with experimental vertical position of the dots was obtained, identifying the horizontal row of three dots at  $E_i = 0.138 \pm 0.01$  eV as the ground vibrational level  $0^0$  of the anion—the anion is thus adiabatically slightly unbound. This number is in good agreement with the value of +0.11 eV derived from an ETS by Burrow *et al.* [17].

*The diagonal patterns.*—The schematic potential curves in Fig. 2 show that a given residual energy is associated with a given change of vibrational quantum  $\Delta n = n - n'$ , the lowest  $E_r$  being associated with  $\Delta n = 0$  for all  $n$ . The residual energy associated with  $\Delta n = 0$  depends only on  $AE_a$ .  $E_r$  of the  $\Delta n = 0$  transitions is the same for all modes

$N$  and they are arranged along the diagonal  $A$  in Fig. 1. When the detachment is regarded as a half collision, then this half collision could be called ‘vibrationally elastic’ along the diagonal  $A$ , since  $n$  and  $n'$  are equal.

Figure 2 shows that this diagonal, extrapolated to  $\Delta E = 0$ , should cross the ‘elastic ridge’ at  $E_i = AE_a$  and this expectation is confirmed by the experiment in Fig. 1. Figure 2 further shows that  $E_r$  should decrease slowly with increasing quanta, the rate of decrease being proportional to the difference of the neutral molecule and anion vibrational energies  $\Delta\nu = \nu - \nu'$ . The diagonal  $A$  should thus slowly approach the threshold line—an expectation confirmed by the experiment.

All dots along the diagonal  $A$  can be satisfactorily assigned to specific transitions. Designating the transitions as  $N^n \rightarrow N'^{n'}$  where  $N$  and  $N'$  are the labels of the modes and  $n$  and  $n'$  the number of quanta of the anion and the neutral molecule, respectively, the leftmost dot is due to the

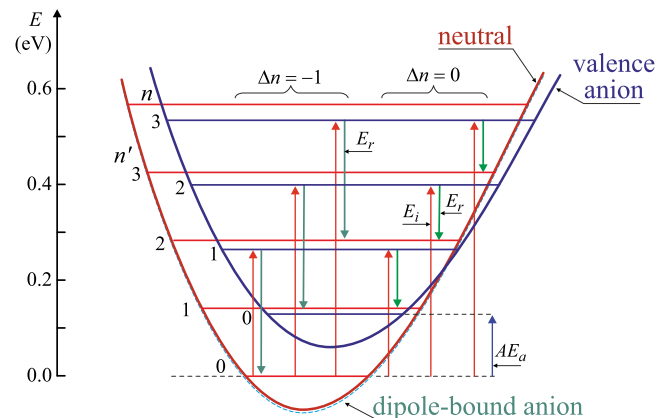


FIG. 2 (color online). Schematic potential curves.

transition  $15^1 \rightarrow 15^1$ , the next as  $10^1 \rightarrow 10^1$ , and similarly for many other modes. Note that dots due to the modes  $\nu_4$ ,  $\nu_5$ , and  $\nu_7$  are slightly below the diagonal because the anion frequencies for these modes are measurably lower than those of the neutral molecule. Dots on the right of the diagonal  $A$  are due to transitions where there is more vibrational energy in the neutral molecule than in the anion—a ‘vibrationally inelastic’ half collision. Examples are the peaks  $0^0 \rightarrow 15^1$ ,  $0^0 \rightarrow 13^1$ ,  $15^1 \rightarrow 15^2$ ,  $9^1 \rightarrow 7^1$ ,  $7^1 \rightarrow 5^1$ , and  $7^1 \rightarrow 5^1 15^1$ .

Dots on the left of the diagonal  $A$  are due to transitions where there is less vibrational energy in the neutral molecule than in the anion—the ‘vibrationally superelastic’ half collisions. Vibrational energy is converted to electronic energy of the departing electron and the process is in that sense related to the vibrational autodetachment studied on nitroalkanes [3] and other anions [4–8] except that in those cases the anions were electronically bound (for example, nitromethane by 172 meV) and vibrational deexcitation was required for the electron to leave; in the present case it is optional and is in competition with the  $\Delta n = 0$  case. Figure 2 shows that for these transitions, with  $\Delta n < 0$ , the vertical separation of a given dot from its pendant on the diagonal  $A$  is equal to the frequency of the vibration which is deexcited. Figure 1 shows that out of the many modes two are dominant, with peaks arranged along two diagonals, labeled  $B$  and  $C$ .

All dots can be assigned to specific transitions. Examples on the diagonal  $B$  are  $7^1 10^1 \rightarrow 10^1$ ,  $7^2 \rightarrow 7^1$ , and  $4^1 7^1 \rightarrow 4^1$ . The vibration deexcited is clearly  $\nu_7$ . Examples on the diagonal  $C$  are  $4^1 10^1 \rightarrow 10^1$ ,  $4^1 7^1 \rightarrow 7^1$ ,  $4^1 5^1 \rightarrow 5^1$ ,  $4^2 \rightarrow 4^1$ , and the vibration deexcited is  $\nu_4$ . There are also weaker dots corresponding to deexcitation of  $\nu_9$  (e.g.,  $4^1 9^1 \rightarrow 4^1$ ) and weak dots at even higher energies which can be assigned to a simultaneous deexcitation of  $\nu_4$  and  $\nu_7$ .

*Discussion and conclusions.*—The 2D spectrum reveals diagonal patterns of the cross section peaks, which are not evident in the more conventional presentation of cross sections. The dominant process is  $\Delta n = 0$ —no change of vibrational quanta during the detachment—leading to the diagonal  $A$  in Fig. 1. Extrapolation of this diagonal to energy loss  $\Delta E = 0$  yields the adiabatic electron attachment energy  $AE_a$ . Many of the remaining peaks are arranged along two other diagonals ( $B$  and  $C$ ), indicating that a large fraction of the remaining processes is accompanied by a highly selective vibrational deexcitation, dominated by only two modes,  $\nu_7$  [C(2)—H(5) rocking] and  $\nu_4$  (C≡N stretch).

The results pose two questions—what is the nature of the resonances and of the autodetachment process? As already pointed out by Burrow *et al.* [17], the observed vibrational origin at +0.138 eV belongs to a shape resonance with a temporary electron capture in the lowest  $\pi^*$  orbital. The present analysis could assign all observed

spectral features to various vibrational states of this shape resonance. This is surprising in the sense that a dipole-bound negative ion has been observed [19] and calculated [20,21], and there is no doubt that vibrationally excited states of this dipole-bound anion are vibrational Feshbach resonances (VFR) [10], which should be accessible by the present experiment. Their absence in the spectra may reflect the low energy-integrated transition probability, possibly related to narrow widths.

With regard to the second question, Simons [12] showed that for a slightly unbound state like the present shape resonance two mechanisms may compete. One is via the direct electronic process, which involves a conventional anion-neutral molecule Franck-Condon factor, weighted by how much the wave function of a given mode samples areas of the potential surface with large widths  $\Gamma(Q)$ . The other is the surface jumping route which proceeds via non-Born-Oppenheimer couplings (and which is the only route for the vibrational autodetachment of anions like  $\text{NH}^-$  that are electronically bound [3–8]). This route does not involve Franck-Condon factors and is similar to the vibrational autoionization which, for potential curves of the same shape leads to a  $\Delta n = \pm 1$  rule [14]. The  $\Delta n = 0$  transitions (on the diagonal  $A$ ) must thus be dominated by the direct electronic process. The  $\Delta n = -1$  processes (diagonals  $B$  and  $C$ ) are much stronger than the  $\Delta n = -2$  processes, and thus follow the  $\Delta n = \pm 1$  rule. The propensity rules formulated for the non-Born-Oppenheimer route by Simons [1,2,12,13,30] are not easy to apply qualitatively to decide whether they can explain the striking  $\nu_4$  and  $\nu_7$  selectivity of the  $\Delta n = -1$  detachment.

It is interesting to compare the present results with the resonant photodetachment experiments [3–8]. The initial steps are different but the detachment is the same. There are important differences, however—photoexcitation is capable of reaching even very narrow resonances, which are not well visible in the electron collision experiment because of the low attachment probability and the IR selection rules limit the number of observable resonances in the photodetachment experiment.

*Outlook.*—Two-dimensional electron energy-loss spectra appear to be a powerful and underappreciated tool to study nuclear dynamics of anions. It would be interesting to apply the present method to larger molecules, where the ‘unselective’ or ‘unspecific’ vibrational excitation related to intramolecular vibrational redistribution [31] is operative near threshold, and would thus appear near the threshold line in the 2D spectrum. It would be interesting to apply the present method to molecules where the dissociative electron attachment channel is also open. An IR photodetachment experiment on the dipole bound acrylonitrile anion would be interesting—it might provide information on the dipole-bound vibrational Feshbach resonances, which are ‘dark’ in the present experiment. Calculations addressing both the direct electronic and the

non-Born-Oppenheimer paths, and both the valence and the VFR anion states, are desirable.

This research is part of Project No. 200020-144367/1 of the Swiss NSF.

- 
- [1] J. Simons, *J. Phys. Chem. A* **112**, 6401 (2008).  
[2] J. Simons, *Adv. Ser. Phys. Chem. B* **10**, 958 (2000).  
[3] C.L. Adams, H. Schneider, and J.M. Weber, *J. Phys. Chem. A* **114**, 4017 (2010).  
[4] C.L. Adams, B.J. Knurr, and J.M. Weber, *J. Chem. Phys.* **136**, 064307 (2012).  
[5] D.M. Neumark, K.R. Lykke, T. Andersen, and W.C. Lineberger, *J. Chem. Phys.* **83**, 4364 (1985).  
[6] K.R. Lykke, D.M. Neumark, T. Andersen, V.J. Trapa, and W.C. Lineberger, *J. Chem. Phys.* **87**, 6842 (1987).  
[7] S.T. Edwards, M.A. Johnson, and J.C. Tully, *J. Chem. Phys.* **136**, 154305 (2012).  
[8] H.K. Gerardi, A.F. DeBlase, C.M. Leavitt, X. Su, K.D. Jordan, A.B. McCoy, and M.A. Johnson, *J. Chem. Phys.* **136**, 134318 (2012).  
[9] G.J. Schulz, *Rev. Mod. Phys.* **45**, 423 (1973).  
[10] H. Hotop, M.-W. Ruf, M. Allan, and I.I. Fabrikant, *Adv. At. Mol. Opt. Phys.* **49**, 85 (2003).  
[11] P.K. Acharya, R.A. Kendall, and J. Simons, *J. Am. Chem. Soc.* **106**, 3402 (1984).  
[12] J. Simons, *J. Am. Chem. Soc.* **103**, 3971 (1981).  
[13] J. Simons, *J. Chem. Phys.* **117**, 9124 (2002).  
[14] R.S. Berry, *J. Chem. Phys.* **45**, 1228 (1966).  
[15] T. Reddish, F. Currell, and J. Comer, *J. Phys. E* **21**, 203 (1988).  
[16] F. Currell and J. Comer, *Phys. Rev. Lett.* **74**, 1319 (1995).  
[17] P.D. Burrow, A.E. Howard, A.R. Johnston, and K.D. Jordan, *J. Phys. Chem.* **96**, 7570 (1992).  
[18] C. Desfrancois, H. Abdoul-Carime, N. Khelifa, and J.P. Schermann, *Phys. Rev. Lett.* **73**, 2436 (1994).  
[19] L. Suess, Y. Liu, R. Parthasarathy, and F.B. Dunning, *J. Chem. Phys.* **119**, 12890 (2003).  
[20] G.L. Gutsev and L. Adamowicz, *J. Phys. Chem.* **99**, 13412 (1995).  
[21] G.L. Gutsev and L. Adamowicz, *Chem. Phys. Lett.* **235**, 377 (1995).  
[22] R.N. Compton, H.S. Carman, C. Desfrancois, H. Abdoul-Carime, J.P. Schermann, J.H. Hendricks, S.A. Lyapustina, and K.H. Bowen, *J. Chem. Phys.* **105**, 3472 (1996).  
[23] T. Sommerfeld and S. Knecht, *Eur. Phys. J. D* **35**, 207 (2005).  
[24] M. Heni and E. Illenberger, *Int. J. Mass Spectrom. Ion Process.* **73**, 127 (1986).  
[25] F.F. Gardner and G. Winnewisser, *Astrophys. J.* **195**, L127 (1975).  
[26] M. Allan, *Phys. Rev. A* **81**, 042706 (2010).  
[27] A.A. Granovsky, Firefly version 8.0.0, <http://classic.chem.msu.su/gran/firefly/index.html>.  
[28] M.W. Schmidt, K.K. Baldrige, J.A. Boatz, S.T. Elbert, M.S. Gordon, J.H. Jensen, S. Koseki, N. Matsunaga, K.A. Nguyen, S. Su *et al.*, *J. Comput. Chem.* **14**, 1347 (1993).  
[29] J.M. Alía, H.G.M. Edwards, W.R. Fawcett, and T.G. Smagala, *J. Phys. Chem. A* **111**, 793 (2007).  
[30] G. Chalasinski, R.A. Kendall, H. Taylor, and J. Simons, *J. Phys. Chem.* **92**, 3086 (1988).  
[31] M. Allan, *J. Electron Spectrosc. Relat. Phenom.* **48**, 219 (1989).